Atomistic simulations of the thermal conductivity of liquids

Marcello Puligheddu[1] and Giulia Galli[1,2,3,*]

[1]*Pritzker School of Molecular Engineering, University of Chicago, Chicago, Illinois 60637, USA*
[2]*Material Science Division, Argonne National Laboratory, Argonne, Illinois 60439, USA*
[3]*Department of Chemistry, University of Chicago, Chicago, Illinois 60637, USA*

(Received 5 November 2019; revised manuscript received 13 March 2020; accepted 21 April 2020; published 11 May 2020)

We present a method based on sinusoidal approach to equilibrium molecular dynamics (SAEMD) to compute the thermal conductivity of liquids. Similar to nonequilibrium molecular dynamics, and unlike equilibrium simulations based on the Green-Kubo formalism, the method only requires the calculation of forces and total energies. The evaluation of heat fluxes and energy densities is not necessary, thus offering the promise of efficiently implementing first principles simulations based on density functional theory or deep molecular dynamics. Our approach is a generalization of SAEMD for solids, where the thermal conductivity is computed in the steady state, instead of a transient regime, thus properly taking into account diffusive terms in the heat equation. We present results for liquid water at ambient conditions and under pressure and discuss simulation requirements to obtain converged values of the thermal conductivity as a function of size and simulation time.

DOI: 10.1103/PhysRevMaterials.4.053801

I. INTRODUCTION

Heat transfer is prevalent in many processes and systems of interest to materials science, chemistry, and geoscience, including electronic devices [1,2], solar [3] and photoelectrochemical cells [4], batteries [5], and transport of fluids in the earth [6]. Hence, the ability to measure and compute the thermal conductivity of solids and liquids is an active field of research. In the past decade, a number of interesting methods have been proposed in the literature to compute the thermal conductivity of solids [7–10], with some of them also applicable to liquids, e.g., molecular dynamics simulations using the Green-Kubo formalism (GK) [11–14] and the (reverse) nonequilibrium MD method (NEMD) [15]. In particular, we recently proposed a method, sinusoidal approach to equilibrium molecular dynamics (SAEMD) [10], which only requires calculations of trajectories and atomic forces; the method avoids the direct computation of heat currents and energy densities necessary within the Green-Kubo approach, which are cumbersome and time consuming to obtain when using first principles calculations. In addition, the method requires shorter sequential simulation times than non equilibrium MD, it can be efficiently used on parallel high performance architectures, and in principle it can be used in conjunction with path integral molecular dynamics methods or ring polymer MD to include quantum effects. However, in its original formulation the SAEMD approach cannot be applied to liquids [10], as discussed in detail below.

Here we present a method based on approach to equilibrium MD simulations, which retains all the advantages of SAEMD, and can straightforwardly be applied to liquids. As an example we present results for liquid water at ambient conditions and under pressure, at conditions (1000 K and 10 GPa) for which *ab initio* simulations of the structural properties of the liquid have been recently reported [16]. Water is responsible for heat transfer in many physical, chemical and biological processes. It exhibits a number of anomalous properties, including high specific heat and, with the exception of liquid metals, the highest thermal conductivity of pure liquids at standard conditions [17]. While measurements of heat transport in water are available at room T and P, very few experiments [18] have been reported under extreme conditions, where the ability to predict thermal conductivity is thus particularly important. The rest of the paper is organized as follows: after a presentation of the method in Sec. II, we present results in Sec. III and our conclusions in Sec. IV.

II. METHOD

The general equation of heat transport is

$$\rho c_p\left[\frac{\partial T}{\partial t} + (\vec{v}\cdot\nabla T)\right] = \kappa\nabla^2 T + \dot{q},$$

where v is the net mass velocity of atoms and molecules in the material, κ is the thermal conductivity, q is the external heat flux, T is the temperature, c_p is the heat capacity at constant pressure (P), and ρ is the density of the system. We compute the thermal conductivity of a condensed system (either fluid or solid) from its response to a perturbation. The latter is expressed as a nonhomogeneous constant temperature profile, which is maintained by a thermostat during a MD simulation. The response of the system results in a nonhomogeneous constant energy flux proportional to the Laplacian of the temperature and to the thermal conductivity. The temperature

*gagalli@uchicago.edu

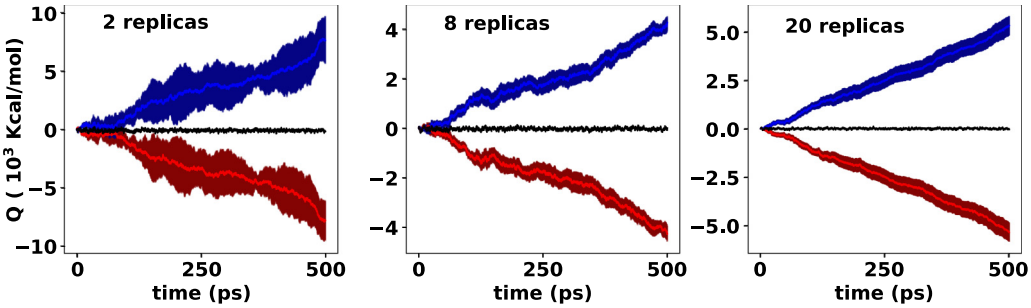

FIG. 1. Energy [$Q(t)$] exchanged between the interior (blue) and exterior (red) partitions of a simulation cell as a function of time, in a close-to-equilibrium molecular dynamics simulation (SAEMD) of liquid water under pressure (see text). The three panels show results obtained by averaging over 2, 8, and 20 replicas. The shaded regions represent the uncertainty in the estimation of $Q(t)$. The black line is the total energy exchanged between the two regions.

profile is defined as:

$$T(x,y,z) = T_0 + \frac{\Delta T}{8}\left\{\left[1-\cos\left(\frac{2\pi x}{L}\right)\right]\left[1-\cos\left(\frac{2\pi y}{L}\right)\right] \times \left[1-\cos\left(\frac{2\pi z}{L}\right)\right] - \frac{1}{2}\right\}, \quad (1)$$

where L is the length of the simulation cell chosen to represent the system, and ΔT is the difference between the maximum and the minimum temperature within the MD cell. When the thermal conductivity is computed using the approach to equilibrium method in a transient regime (SAEMD method), $q = 0$ and the velocity term v is set to zero, to obtain

$$\frac{\partial T}{\partial t} = \frac{\kappa}{\rho c_p}\nabla^2 T.$$

In the case of solids, setting $v = 0$ is justified, since the atoms are not free to move. However, in the case of liquids, atoms, or molecules diffuse and the velocity term cannot be set to zero. Hence, to generalize the SAEMD method to liquids, here we solve the heat equation in the presence of a perturbation *in the steady state*, where

$$0 = \kappa\nabla^2 T + \dot{q}.$$

We partition the MD cell into two regions, an interior one defined as the sphere centered in the middle of the cell and containing half of its volume; the second region (exterior) contains the remaining half of the cell. This partition is not unique, and the system may be divided into more than two regions, if needed. Our choice is motivated by the simplicity of the configuration.

After the perturbation is applied, we monitor how much energy the thermostat is providing to the interior region, and how much energy the thermostat removes from the exterior one. This continuous energy exchange is necessary to maintain the temperature difference between the two regions in the steady state and the sum of the energy provided and removed must be zero when a steady state is reached. The time derivative of the difference of the energy exchanged ($\dot{q}$) is the key quantity necessary for the calculation of the thermal conductivity.

Under the assumption that the thermal conductivity (κ) of the system is isotropic and independent on position, we can obtain κ from the ratio of $\dot{q}$ and the difference in the integrals over the two regions (internal and external) of the Laplacian of the temperature We note that, depending on the size of the chosen simulation cell and hence on the temperature gradient created in the cell, the temperature profile obtained during the simulation may turn out not to be identical to the one specified by the perturbation imposed. Hence in order to correct for this behavior,in our calculations we multiplied the difference in the integrals of Eq. 2 by the ratio between the expected temperature difference in the two regions and the one observed during the simulation [19]:

$$\dot{q} = \frac{\partial(q_{\text{int}} - q_{\text{ext}})}{\partial t} = \kappa\left(\int_{\text{int}}\nabla^2 T - \int_{\text{ext}}\nabla^2 T\right). \quad (2)$$

To obtain statistically meaningful data, in our simulations we averaged over results obtained from multiple independent replicas. We show the importance of using multiple replicas in Fig. 1, where we report q_{int}, q_{ext} and their estimated error as a function of the simulation time using 2, 8, and 20 replicas for the calculations of the thermal conductivity of water under pressure, using cells with 512 water molecules at $P = 9.7$ GPa and $T = 1000$ K.

The thermal conductivity computed from MD simulations using periodic boundary conditions (pbc) suffers from finite-size effects for two reasons: (i) the cell size (and hence number of atoms) chosen to represent the heat propagation in the system is of course finite; this approximation is present in all methods and it is the only source of finite-size effects in equilibrium simulations based on GK; (ii) the need to keep different parts of the system at different T, to monitor the flow of energy; this approximation affects the NEMD and SAEMD approaches, but clearly not GK.

Due to the presence of finite-size effects, an extrapolation of simulation results obtained for different cell sizes is usually necessary to obtain a converged value of κ. In solids, the extrapolation of simulation results as a function of size is obtained using models for phonon mean free paths [20,21]. In liquids, simple models of vibrational modes and their mean free path are not available. We derived approximate formulas to extrapolate the results of our simulations for water based on the phenomenological model of heat transport presented in reference [22], where the contribution of all pairs of molecules

up to a distance r to the heat flux (J) is written as

$$J(r) = C\rho_N^2 \int_0^r \dot{Q}(r')g(r')r'^3 r'^{-m} dr'. \quad (3)$$

Here g is the radial distribution function of the liquid, C is a constant, ρ_N is the number density; r^{-m} accounts for the fact that the interaction between molecules is a many-body interaction, rather than pair-wise. For liquid water in the range 300–600 K, using MD simulations Ohara [22] found that $\dot{Q}(r') = Q_0/r^3$ for $r > 0.7$ nm and that a value of $m = 2$ best describes the heat flux of water at ambient conditions. In the limit of large r, $g(r) = 1$ and we rewrite Eq. (3) as

$$J(L) = J_\infty - C' \int_L^\infty Q_0 r^{-2} dr = J_\infty(1 - \lambda/L), \quad (4)$$

where J_∞ is the extrapolated value of the heat current for $L \to \infty$ and C and λ are constants. In our simulations we observed that the autocorrelation function $[A(\tau)]$ of the current $J(t)$ can be expressed as a product of an oscillating function independent on size $[f(\tau)]$ multiplied by size dependent intensities and we approximate it as $A(\tau) \simeq (J_L)^2 f(\tau)$. Hence, the thermal conductivity is proportional to $(J_L)^2$ and using Eq. (4) we write κ as

$$\kappa(L) = C'' J_\infty (1 - \lambda/L)^2 = \kappa_\infty (1 - \lambda/L)^2, \quad (5)$$

where κ_∞ is the extrapolated value of the thermal conductivity for $L \to \infty$ and C'' is a constant. As we will see below, using Eq. (5) we can accurately fit our simulation results at ambient conditions and thus determine the value of κ_∞. However, as expected, Eq. (5) is not appropriate to fit our high T and P results, since the value $m = 2$ used in Eqs. (4) and (5) was derived for water at ambient conditions. Hence, we rewrote Eq. (5) by treating m as a fitting parameter and we found that a value of $m = 4$ appeared to fit our simulation results relatively well. For $m = 4$ Eq. (5) becomes to leading order in $1/L$,

$$\kappa(L) = \kappa_\infty (1 - (\lambda/L)^3), \quad (6)$$

and as shown below it fits accurately our high pressure results. We note that Eq. (5) is equal to leading order in L to an equation [23] derived from hydrodynamics arguments and used to describe finite-size effects in the calculations of the diffusivity of fluids, including water. We now turn to the presentation of our results.

III. RESULTS

In this section we present our results for the thermal conductivity of water at ambient conditions ($T = 300$ K, $\rho = 1$ g/cm^3) and under pressure ($T = 1000$ K, $\rho = 1.57$ g/cm^3). Structural properties under pressure were recently investigated [16] with *ab initio* MD using the PBE functional [24], and we chose one snapshot from the trajectories reported in the *ab initio* study to start our simulations. Water at ambient conditions was described with the TIP4P-2005f force field [25]. This empirical potential turned out to be numerically unstable at high T and P; in particular, we found non physical dissociation events in our simulations. At high P we then used the SPCE-Fl force field [26], which describes the OH bonded interaction with a harmonic potential and by construction cannot lead to any dissociation. Note that we used flexible potentials to avoid spurious effects in the calculations of heat transfer brought about by the presence of constraints in MD simulations with rigid water molecules [27]. As discussed in the conclusions, it would be desirable to use more realistic force fields and ultimately conduct *ab initio* simulations; however as reported below, the time scales required for the simulations of heat transport in water make the use of *ab initio* MD prohibitive and point at the future use of machine-learned first principle potentials as a viable alternative. In our work we chose to use empirical potentials to demonstrate the accuracy and robustness of the method proposed here, as compared to GK simulations, and to test finite-size scaling and the required simulation times.

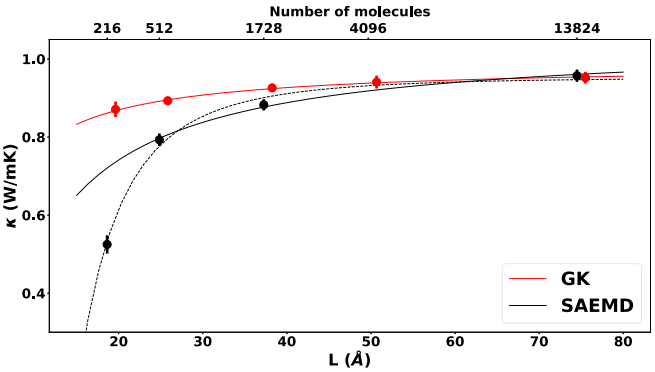

FIG. 2. Thermal conductivity (κ) of water at 300 K as a function of the linear size (L) of the cubic simulation cell and the number of water molecules. Results obtained with Green-Kubo (GK) and close-to-equilibrium molecular dynamics simulations (SAEMD) are represented by red and black dots, respectively. Solid lines were obtained by fitting the data with Eq. (5). We also show a fit of SAEMD results using Eq. (6) (dotted black line). All simulations were performed with the TIP4P-2005f force field. GK results are slightly offset on the x axis to avoid overlap with SAEMD results.

We compare below (Figs. 2 and 3) results obtained with GK and SAEMD simulations. In the former case, for each replica we carried out simulations for 800 000 steps (200 ps) under NVT conditions (initializing the calculation with different initial velocities in different replicas), followed by NVE simulations to collect data to compute the thermal conductivity. When discussing simulation time we only refer to this part of the simulation. For each cell size we used eight replicas and 600 ps long simulations, except for the 13 824 molecule cell, where we run four replicas.

The SAEMD simulations included three steps: (i) equilibration of the system at constant temperature; (ii) application of a temperature perturbation; we carried out relatively long simulations of about 100 ps in this transient regime but several tests indicated that if needed, this time may be decreased by up to one order of magnitude, the exact simulation time depending on the system; (iii) collection of results to compute κ. As in the case of Green-Kubo simulations, we averaged over multiple independent replicas and when discussing simulation time we only refer to the final part of the simulation.

Figure 2 shows our results for the thermal conductivity of water at 300 K, 1 g/cm^3 using the TIP4P-20005f potential, computed using Green-Kubo and SAEMD simulations. Both

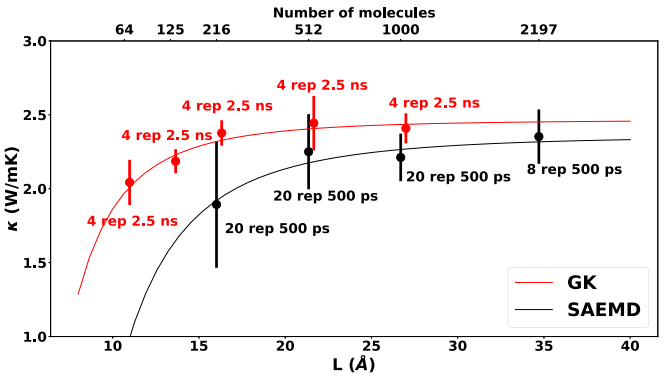

FIG. 3. Thermal conductivity (κ) of water at 1000 K and a density of 1.57 g/cm^3 as a function of the linear size (L) of the cubic simulation cell and the number of water molecules. Results obtained with Green-Kubo (GK) and close-to-equilibrium molecular dynamics simulations (SAEMD) are represented by red and black dots, respectively. Solid lines were obtained by fitting the data with Eq. (6). All simulations were performed with the SPCE-Fl force field. GK results are slightly offset on the x axis to avoid overlap with SAEMD results.

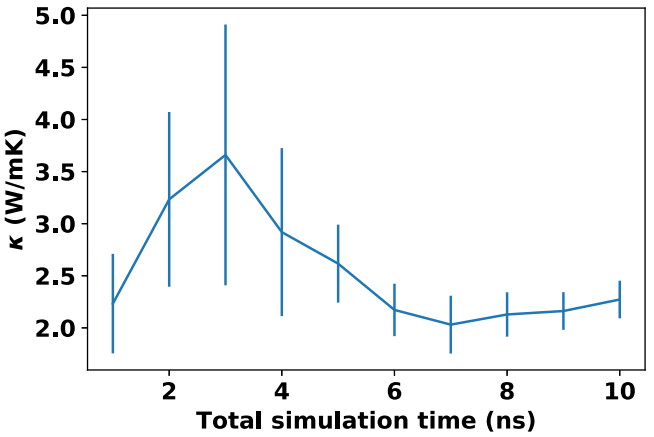

FIG. 4. Thermal conductivity (κ) of water at 1000 K and a density of 1.57 g/cm^3 computed with a 512 molecule cell by close-to-equilibrium molecular dynamics simulations, as a function of the total simulation time. All simulations were performed with the SPCE-Fl force field.

methods yield almost identical extrapolated values of the thermal conductivity, within error bars: we obtained 0.98 ± 0.01 for GK and 0.95 ± 0.02 for SAEMD when using Eq. (6) to fit the data and 1.04 ± 0.01 when using Eq. (5) to fit only three points. GK results were extrapolated using Eq. (5). We note that GK simulation results exhibit a weaker dependence on size: for example in simulations with 512 water molecules, the GK value of κ is about 10% lower than κ_∞, while that obtained with SAEMD is about 16% lower. We emphasize that while GK appears to be the method of choice when using empirical potentials, due to its weaker size dependence, the SAEMD approach offers the promise of efficiently performing simulations with neural-network-derived potentials and possibly using forces derived from DFT, since it does not require any calculation of the heat flux or of energy densities but only of energies and forces.

In Fig. 3 we present our results for water at 1000 K, and 9.7 GPa using the SPCE-Fl force field. The values of the thermal conductivity extrapolated using Eq. (6) are 2.47 ± 0.04 and 2.36 ± 0.06 for GK and SAEMD, respectively. As in the case of water at ambient conditions, size effects are more severe when using SAEMD, although in this case the two methods give the same results within statistical error bars for 512 molecule simulations. The increase of more than a factor of 2 of the thermal conductivity found here at extreme conditions is consistent with the observed increase of thermal conductivity of water with respect to pressure [28].

In Fig. 4 we show the thermal conductivity as a function of the total simulation time in a SAEMD simulation, when using 512 water molecule cells at 1000 K, computed by averaging over 20 replicas, each simulated for 500 ps. We found that for a total simulation time equal to or larger than 5 ns, the results are approximately converged. In Fig. 5 we show the relative error in the thermal conductivity of water at 1000 K using 512 molecules as a function of the number of replicas used and of the simulation time. The figure shows that, after a short simulation time of 100 ps, the error can be reduced by either increasing the simulation time or the number of replicas. While the total simulation time is the same for the same relative error, the option of increasing the number of replicas allows for independent parallel runs and shorter sequential times.

In Table I we summarize available results for the thermal conductivity of water at $\approx$ 300 K and 1 atm. None of the values reported in the table, except those obtained here, were extrapolate to obtain κ_∞ although some studies did increase the number of molecules in the cell in the direction of heat transport to test finite-size effects. Overall we expect the values obtained with small cell sizes to be an underestimate of the extrapolated value for a given force-field; hence the apparent agreement with experiments is not necessarily representative of the accuracy of the force field or in general of the description of the interaction chosen in the simulations.

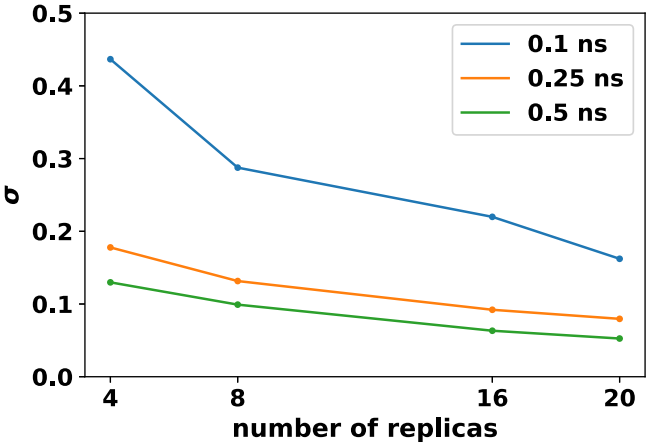

FIG. 5. Average relative error (σ) in the computed thermal conductivity of water at 1000 K and density of 1.57 g/cm^3, as a function of the number of replicas. Simulations were carried out with 512 molecule cells and the close-to-equilibrium approach, using the SPCE-Fl force field.

TABLE I. Measured (Exp) and computed values of the thermal conductivity [κ (W/mK)] of water at density of $\simeq 1$ g/cm^3, obtained using different force fields (first column). All computed values were obtained using molecular dynamics with the Green-Kubo (GK), nonequilibrium (NEMD), or close-to-equilibrium (SAEMD) approach (see second column) at a temperature [T (K)] given in the third column. The maximum number of molecules ($N_{\rm mol}$) in the unit cell, the simulation time per replica (t_s), and the number of replicas ($N_{\rm rep}$ are given in columns 5, 6, and 7, respectively.

Force field	Method	T	κ	$N_{\rm mol}$	t_s	$N_{\rm rep}$	Ref.
TIP4P-2005f [25]	GK	300 K	0.98(1)	13 824	600 ps	4	This work
TIP4P-2005f	SAEMD	300 K	0.95(2)	13 824	500 ps	4	This work
SPC [29]	NEMD	298 K	0.88(2)	900	2 ns	1	[30]
SPC	NEMD	298 K	0.776(19)	2180	1 ns	1	[31]
SPC	GK	298 K	0.802(16)	2180	1 ns	1	[31]
SPCE [32]	NEMD	298 K	0.930(16)	900	2 ns	1	[30]
SPC f [29,33]	NEMD	300 K	0.7(1)	27 036	300 ps	1	[33]
SPCE-F [34]	GK	300 K	0.970(9)	180	40 ns	1	[35]
SPC-Fw [36]	GK	300 K	0.854(104)	2180	1 ns	1	[31]
SPC-Fw	NEMD	300 K	1.011(6)	2180	1 ns	1	[31]
SPC-Fd [37]	GK	300 K	0.793(105)	2180	1 ns	1	[31]
SPC-Fd	NEMD	300 K	0.977(12)	2180	1 ns	1	[31]
TIP3P [38]	NEMD	298 K	0.880(19)	900	2 ns	1	[30]
TIP4P-2005 [39]	NEMD	298 K	0.910(14)	900	2 ns	1	[30]
TIP5P [40]	GK	298 K	0.668(31)	2048	15–20 ns	6	[41]
TIP5P	NEMD	298 K	0.680(7)	900	2 ns	1	[30]
TIP5P-Ew [42]	NEMD	298 K	0.620(7)	900	2 ns	1	[30]
PBE [24]	GK	385 K	0.74(12)	64	90 ps	1	[7]
PBE [24]	NEMD	353 K	0.79	480	150 ps	1	[43]
Exp		300 K	0.609				[44]
Exp		300 K	0.6096				[45]

IV. CONCLUSIONS

We presented a method for the calculation of the thermal conductivity of liquids which relies on molecular dynamics simulations conducted close-to-equilibrium conditions, in the steady state. Similar to nonequilibrium molecular dynamics, and unlike equilibrium simulations based on GK, the method only requires the calculation of forces and total energies and the evaluation of heat fluxes and energy densities is not necessary. The close-to-equilibrium approach requires in general shorter simulation times than NEMD and thus allows one to take better advantage of parallel computing architectures. However, the cell-size dependence found in the present work is still less favorable than that observed with GK simulations. Hence, when using empirical force fields, for which the calculation of energy densities is straightforward and does not add any computational complexity, GK simulations should be the method of choice for homogeneous systems, from the standpoint of efficiency. Instead, in cases when computing energy densities and heat fluxes amount to additional, expensive calculations (as, e.g., in the case of first-principles simulations), SAEMD is expected to be the most efficient method for solid and the method presented here the most efficient one for liquids. We note, however, that, at least in the case of liquid water and ambient and extreme conditions studied here, the cell sizes and especially simulation times required for convergence still rule out the possibility of carrying out converged first principles simulations (and the same is true for GK). We expect that the ionic component of the thermal conductivity of liquid metals and possibly other fluids at elevated temperatures may be computed using the method presented here and DFT derived forces. An interesting direction to explore is the use of the approach in conjunction with deep-MD potentials based on first principles forces [46]. In fact, we have successfully conducted a simulation of a 512 molecule cell of water molecules at high pressure and temperature using the deep-MD potential developed with the method of Ref. [46] and the close-to-equilibrium approach. Work is in progress to perform simulations with the same potential for several other conditions under pressure, so as to predict the thermal conductivity of water at extreme conditions, where experiments are still rather challenging to perform. The results obtained here with empirical potentials show a more than two-fold increase of the thermal conductivity of water when going from 300 K to high pressure and temperature conditions ($P \simeq 10$ GPa and $T \simeq 1000$ K). Finally, we note that in the case of water, especially at ambient conditions, proton quantum effects are likely to play a significant role in determining the value of the thermal conductivity and that close-to-equilibrium simulations are expected to be more straightforward to couple to a path integral formulation than simulations based on the Green-Kubo formalism.

Data and workflows are available at [47].

ACKNOWLEDGMENTS

We thank F. Gygi, L. Zhang, and R. Car for helpful discussions. This work was supported by MICCoM, as part of the Computational Materials Sciences Program funded by the U.S. Department of Energy, Office of Science, Basic Energy Sciences, Materials Sciences and Engineering Division.

[1] S. V. Garimella, T. Persoons, J. A. Weibel, and V. Gektin, IEEE Trans. Compon. Packag. Manuf. Technol. **7**, 1191 (2017).

[2] E. Pop, Nano Res. **3**, 147 (2010).

[3] A. Ndiaye, A. Charki, A. Kobi, C. M. Kébé, P. A. Ndiaye, and V. Sambou, Sol. Energy **96**, 140 (2013).

[4] S. Tembhurne, F. Nandjou, and S. Haussener, Nature Energy **4**, 399 (2019).

[5] Y. Zhu, J. Xie, A. Pei, B. Liu, Y. Wu, D. Lin, J. Li, H. Wang, H. Chen, J. Xu, A. Yang, C.-L. Wu, H. Wang, W. Chen, and Y. Cui, Nat. Commun. **10**, 2067 (2019).

[6] A. G. Whittington, A. M. Hofmeister, and P. I. Nabelek, Nature **458**, 319 (2009).

[7] A. Marcolongo, P. Umari, and S. Baroni, Nat. Phys. **12**, 80 (2015).

[8] C. Carbogno, R. Ramprasad, and M. Scheffler, Phys. Rev. Lett. **118**, 175901 (2017).

[9] D. A. Broido, M. Malorny, G. Birner, N. Mingo, and D. A. Stewart, Appl. Phys. Lett. **91**, 231922 (2007).

[10] M. Puligheddu, F. Gygi, and G. Galli, Phys. Rev. Mater. **1**, 060802 (2017).

[11] M. S. Green, J. Chem. Phys. **20**, 1281 (1952).

[12] M. S. Green, J. Chem. Phys. **22**, 398 (1954).

[13] R. Kubo, M. Yokota, and S. Nakajima, J. Phys. Soc. Jpn. **12**, 1203 (1957).

[14] R. Kubo, J. Phys. Soc. Jpn. **12**, 570 (1957).

[15] F. Müller-Plathe, J. Chem. Phys. **106**, 6082 (1997).

[16] V. Rozsa, D. Pan, F. Giberti, and G. Galli, Proc. Natl. Acad. Sci. USA **115**, 6952 (2018).

[17] R. C. Reid, J. M. Prausnitz, and B. E. Poling, *The Properties of Gases and Liquids* (McGraw Hill, New York, NY, 1987).

[18] Z. M. Geballe and V. V. Struzhkin, J. Appl. Phys. **121**, 245901 (2017).

[19] We note that, depending on the size of the chosen simulation cell and hence on the temperature gradient created in the cell, the temperature profile obtained during the simulation may turn out not to be identical to the one specified by the perturbation imposed. Hence, to correct for this behavior, in our calculations we multiplied the difference in the integrals of Eq. (2) by the ratio between the expected temperature difference in the two regions and the one observed during the simulation.

[20] P. K. Schelling, S. R. Phillpot, and P. Keblinski, Phys. Rev. B **65**, 144306 (2002).

[21] H. Zaoui, P. L. Palla, F. Cleri, and E. Lampin, Phys. Rev. B **94**, 054304 (2016).

[22] T. Ohara, J. Chem. Phys. **111**, 6492 (1999).

[23] I.-C. Yeh and G. Hummer, J. Phys. Chem. B **108**, 15873 (2004).

[24] J. P. Perdew, K. Burke, and M. Ernzerhof, Phys. Rev. Lett. **77**, 3865 (1996).

[25] M. A. González and J. L. F. Abascal, J. Chem. Phys. **135**, 224516 (2011).

[26] J. López-Lemus, G. A. Chapela, and J. Alejandre, J. Chem. Phys. **128**, 174703 (2008).

[27] T. M. Yigzawe and R. J. Sadus, J. Chem. Phys. **138**, 044503 (2013).

[28] B. Chen, W.-P. Hsieh, D. G. Cahill, D. R. Trinkle, and J. Li, Phys. Rev. B **83**, 132301 (2011).

[29] W. F. v. G. H. J. C. Berendsen, J. P. M. Postma and J. Hermans, in *Intermolecular Forces*, edited by B. Pullman and D. Reidel (D. Reidel Publishing Company, The Netherlands, 1981).

[30] Y. Mao and Y. Zhang, Chem. Phys. Lett. **542**, 37 (2012).

[31] T. W. Sirk, S. Moore, and E. F. Brown, J. Chem. Phys. **138**, 064505 (2013).

[32] H. J. C. Berendsen, J. R. Grigera, and T. P. Straatsma, J. Phys. Chem. **91**, 6269 (1987).

[33] W. Evans, J. Fish, and P. Keblinski, J. Chem. Phys. **126**, 154504 (2007).

[34] J. Alejandre, G. A. Chapela, F. Bresme, and J.-P. Hansen, J. Chem. Phys. **130**, 174505 (2009).

[35] L. Ercole, A. Marcolongo, and S. Baroni, Sci. Rep. **7**, 15835 (2017).

[36] Y. Wu, H. L. Tepper, and G. A. Voth, J. Chem. Phys. **124**, 024503 (2006).

[37] L. X. Dang and B. M. Pettitt, J. Phys. Chem. **91**, 3349 (1987).

[38] W. L. Jorgensen, J. Chandrasekhar, J. D. Madura, R. W. Impey, and M. L. Klein, J. Chem. Phys. **79**, 926 (1983).

[39] J. L. F. Abascal and C. Vega, J. Chem. Phys. **123**, 234505 (2005).

[40] M. W. Mahoney and W. L. Jorgensen, J. Chem. Phys. **112**, 8910 (2000).

[41] N. J. English and J. S. Tse, J. Phys. Chem. Lett. **5**, 3819 (2014).

[42] S. W. Rick, J. Chem. Phys. **120**, 6085 (2004).

[43] E. Tsuchida, J. Phys. Soc. Jpn. **87**, 025001 (2018).

[44] R. W. Powell, C. Y. Ho, and P. E. Liley, NIST Reference Data 130 (1966).

[45] M. L. V. Ramires, C. A. Nieto de Castro, Y. Nagasaka, A. Nagashima, M. J. Assael, and W. A. Wakeham, J. Phys. Chem. Ref. Data **24**, 1377 (1995).

[46] L. Zhang, J. Han, H. Wang, R. Car, and W. E, Phys. Rev. Lett. **120**, 143001 (2018).

[47] M. Puligheddu and G. Galli, "Atomistic simulations of the thermal conductivity of liquids", https://paperstack.uchicago.edu/paperdetails/5eb086e8e092384bb26754dc (2020).